



Published in final edited form as:

*Biomed Pharmacother.* 2023 May ; 161: 114514. doi:10.1016/j.biopha.2023.114514.

## Piceatannol induces regulatory T cells and modulates the inflammatory response and adipogenesis

**Ahmed Rakib<sup>a,1</sup>, Mousumi Mandal<sup>a,1</sup>, Anaum Showkat<sup>a</sup>, Sonia Kiran<sup>a</sup>, Soumi Mazumdar<sup>b</sup>, Bhupesh Singla<sup>a</sup>, Aman Bajwa<sup>c,d</sup>, Santosh Kumar<sup>a</sup>, Frank Park<sup>a</sup>, Udai P. Singh<sup>a,\*</sup>**

<sup>a</sup>Department of Pharmaceutical Sciences, College of Pharmacy, The University of Tennessee Health Science Center, Memphis, TN, USA

<sup>b</sup>Department of Physiology, College of Medicine, The University of Tennessee Health Science Center, Memphis, TN, USA

<sup>c</sup>Transplant Research Institute, James D. Eason Transplant Institute, Department of Surgery, College of Medicine, The University of Tennessee Health Science Center, Memphis, TN, USA

<sup>d</sup>Department of Genetics, Genomics, and Informatics, College of Medicine, The University of Tennessee Health Science Center, Memphis, TN, USA

### Abstract

The beneficial effects of the polyphenolic compound piceatannol (PC) has been reported for metabolic diseases, antiproliferative, antioxidant, and anti-cancer properties. Despite its beneficial effects on inflammatory diseases, little is known about how PC regulates inflammatory responses and adipogenesis. Therefore, this study was designed to determine the effects of PC on the inflammatory response and adipogenesis. The effect of PC on splenocytes, 3T3-L1 adipocytes, and RAW264.7 macrophages was analyzed by flow cytometry, qRT-PCR, morphometry, and western blot analysis. PC induced apoptosis in activated T cells in a dose-dependent manner using stimulated splenocytes and reduced the activation of T cells, altered T cell frequency, and interestingly induced the frequency of regulatory T (Treg) cells as compared to controls. PC suppressed the expression of TNF- $\alpha$ , iNOS, IL-6R, and NF- $\kappa$ B activation in RAW264.7 macrophages after lipopolysaccharides (LPS)-induction as compared to the control. Interestingly,

---

This is an open access article under the CC BY-NC-ND license (<http://creativecommons.org/licenses/by-nc-nd/4.0/>).

\*Corresponding author.: [usingh1@uthsc.edu](mailto:usingh1@uthsc.edu) (U.P. Singh).

<sup>1</sup>These authors contributed equally to this manuscript

#### Conflict of Interest Statement

The all authors declare that they do not have any competing interests that might influence this study and have had no involvement with study sponsors.

#### Ethics Statement

All animal experimentation was performed under a protocol number (UPS 20–0169) approved by the University of Tennessee Health Science Center (UTHSC) Institutional Animal Care and Use Committee (IACUC). All animal handling and experimental procedures involving animals were performed to minimize pain and discomfort.

#### CRedit authorship contribution statement

**Ahmed Rakib, Mousumi Mandal, Anaum Showkat, Sonia Kiran, and Soumi Mazumdar:** Data curation, performed the majority of the experiments, and data analysis. **Ahmed Rakib, Mousumi Mandal:** wrote the first draft of the manuscript and made all the figures. **Aman Bajwa, and Bhupesh Singla:** provided the cell lines, helped with data analysis, and critically edited the manuscript. **Santosh Kumar and Frank Park:** Assisted with editing the manuscript. **Udai Singh:** Conceived the idea, review and edited the manuscript.

PC altered the cell morphology of 3T3-L1 adipocytes with a concomitant decrease in cell volume, lipid deposition, and TNF- $\alpha$  expression, but upregulation of leptin and IL-1 $\beta$ . Our findings suggested that PC induced apoptosis in activated T cells, decreased immune cell activation and inflammatory response, and hindered adipogenesis. This new set of data provides promising hope as a new therapeutic to treat both inflammatory disease and obesity.

## Keywords

Piceatannol (PC); Regulatory T (Treg) cells; Inflammation; Macrophage; Adipogenesis

---

## 1. Introduction

Piceatannol (PC) (3,4',3',5-trans-trihydroxystilbene) is a stilbene and a resveratrol analog, which is commonly found in red grapes, wines, passion fruit, Japanese knotweed, and Asian legumes [1,2]. Although resveratrol has beneficial effects on chronic diseases, it has poor bioavailability and rapid metabolism [3]. To overcome this issue, several analogs of resveratrol, including PC, have been studied to determine their effect on inflammatory diseases. Studies have reported that PC has exhibited anti-cancer, anti-inflammatory, and antioxidant activities [2,4,5], but the mechanism is not clear. In addition to this, it has been reported that PC mediates tumor necrosis factor- $\alpha$  (TNF- $\alpha$ ) mediated inflammation and inhibits the production of prostaglandin 2 (PGE2), and nitric oxide (NO) by modulating transcription factor nuclear factor kappa B (NF- $\kappa$ B) and CCAAT-enhancer-binding proteins (C/EBP) in RAW264.7 macrophage cell lines [6]. Recently, it was shown that PC exerts anti-obesity effects in mice through modulating adipogenic proteins and gut microbiota [7]. Further, PC inhibits adipogenesis by modulating mitotic clonal expansion and insulin-dependent signaling in the early phase of adipocyte differentiation [8]. However, the mechanism of how PC exerts its anti-inflammatory effects and modulates adipogenesis remains to be fully determined.

Inflammation is considered a protective mechanism of the body, in which the immune system defends the body from harmful agents like bacteria and viruses. If inflammation persists for a long time, it causes chronic inflammation and is related to the production and secretion of several pro-inflammatory mediators. These mediators are associated with abnormal perturbation of the native immune response from normal homeostasis and play a crucial role in promoting various types of organ injuries and diseases [9]. Chronic inflammation leads to many autoimmune diseases such as inflammatory bowel disease (IBD), Type 1 Diabetes (T1D), and obesity and is currently a growing health concern around the world. Thereby, chronic inflammation should be controlled appropriately in time to protect from various diseases. To date, available drugs that suppress inflammation have limited efficacy with many side effects, thereby identifying new natural anti-inflammatory agents for the treatment of inflammatory disorders is a provocative area of therapeutic need. Towards achieving this goal, PC possesses various pharmacological attributes, including anti-inflammatory properties, and it has been used for the treatment of several disease conditions including cancer, liver injury, and skin diseases [3,10,11].

Various immune cells, including T cells and macrophages play a key role in the regulation of inflammation as well as being responsible for controlling autoimmune diseases. Towards this end, macrophages are one of the most dominant and widely distributed inflammatory cells associated with the initiation and regulation of acute and chronic inflammatory responses [12]. Lipopolysaccharide (LPS), which is the major component of the outer membrane of Gram-negative bacteria, are important for triggering a cascade of processes related to inflammatory immune responses mediated by toll-like receptor (TLR) signaling. A previous study demonstrated that PC treatment suppressed the secretion of proinflammatory cytokines and NO synthesis in RAW264.7 macrophage cells after LPS induction [13].

The transcriptional factor NF- $\kappa$ B is regarded as a master regulator of several inflammatory genes [14]. After activation, NF- $\kappa$ B initiates the expression of pro-inflammatory genes and further extremely accumulates various pro-inflammatory mediators, including TNF- $\alpha$ , interleukin (IL)-1 $\beta$ , IL-6, and NO [15,16]. Inhibiting the activities of NF- $\kappa$ B can effectively attenuate inflammatory conditions and decreases the progression of the disease. Further, TNF- $\alpha$  secreted from macrophages and T cells infiltrate adipose tissue, thereby increase the risk factors for obesity-related metabolic disorders [6]. However, a study reported that PC significantly suppressed the expression of both TNF- $\alpha$  and IL-6 in NIH3T3-L1 cells [13]. Further, PC represents anti-lipolytic function, which is crucial since obesity is related to the potential increase in basal lipolysis [17,18]. Despite numerous beneficial effects, little is known about how PC affects the inflammatory response and adipogenesis.

In this present study, we investigated the effects of PC on the inflammatory response and modulation of adipocyte function using splenocytes, RAW264.7 macrophages, and NIH3T3-L1 cells by in vitro analysis.

## 2. Materials and methods

### 2.1. Splenocyte single cell isolation and PC treatment

Wild-type C57BL/6J male mice (7 weeks of age) were purchased from Jackson Laboratories (Bar Harbor, ME) and housed in the animal facility at the University of Tennessee Health Science Center (UTHSC). The mice were kept with a normal 12:12 h light/dark cycle with ad libitum access to food and water for a week to acclimate them to the animal facility under humidity and temperature-controlled conditions. Experiments were performed under an approved protocol (# 20–0169) by the University of Tennessee Health Science Centre (UTHSC) Institutional Animal Care and Use Committee (IACUC). After euthanization, spleens were collected from the mouse and dissociated by a Stomacher (Seward Stomacher<sup>®</sup> 80) to make single-cell suspensions. Red blood cells (RBCs) were removed by RBC lysis buffer (Cat. No. 00–4333–57, Invitrogen, Waltham, MA). After RBC lysis, cells were centrifuged at  $300 \times g$  for 8 min, the supernatant was discarded, and the cells were suspended in Roswell Park Memorial Institute (RPMI)–1640 medium (Cat. No. 10–041-CV, Corning, NY) containing 10 % fetal bovine serum (FBS) (Cat. No. 25–550 H, Genesee Scientific, San Diego, CA). Initially, a day before the experiment, individual 6-well plates were coated with anti-CD3 antibody (5  $\mu$ g/mL; clone: 145–2C11, Catalog No. 100360, BioLegend, San Diego, CA) and kept overnight at 4°C. In the experiment, single-cell suspensions of splenocytes were seeded in each well of the 6-well plates ( $1.5 \times 10^6$  cells/

well). The cells were treated with an anti-CD28 antibody (1  $\mu\text{g}/\text{mL}$ ; Clone: 37.51, Cat. No. 102116, BioLegend, San Diego, CA) along with 10  $\mu\text{M}$  PC (Cat. No. 1554/10; R&D Systems, Minneapolis, MN) or without (control) and incubated for 72 h at 37°C, 5 %  $\text{CO}_2$  incubator. PC is safe and we did not notice any cytotoxicity in our in vitro experiments.

## 2.2. RAW264.7 and NIH3T3-L1 cell culture and treatment

RAW264.7 mouse macrophage cells (ATCC TIB-71) were cultured in Dulbecco's modified essential medium (DMEM) (Cat. No. 8921008, Corning, NY) media supplemented with 10 % heat-inactivated FBS, penicillin/streptomycin (100 U/mL/100  $\mu\text{g}/\text{mL}$ ) (Cat. No. 15140–122, Gibco, Waltham, MA) and maintained at 37°C, in 5 %  $\text{CO}_2$  incubator. Media was replaced every 48 h for the duration of the experiment. In all experiments, RAW264.7 macrophages were treated in the presence or absence (control) of 10  $\mu\text{M}$  PC added with 100 ng/mL lipopolysaccharide (Cat. No. L4391, Sigma, St. Louis, MO) for 24 h.

3T3-L1 (ATCC-CL-173) preadipocyte cells were cultured and maintained in DMEM supplemented with L-glutamine (2 mM) (Cat. No. 25030–081, Gibco, Waltham, MA), sodium pyruvate (1 mM) (Cat. No. 11360–070, Gibco, Waltham, MA), penicillin/streptomycin (100 U/mL/100  $\mu\text{g}/\text{mL}$ ), and 10 % fetal calf serum (FCS) (Cat. No. 26010–066, Gibco, Waltham, MA). Preadipocytes were passaged upon reaching 70 % confluence. For differentiation into adipocytes, 3T3-L1 cells were grown to confluency, at this point media was replaced with DMEM supplemented with L-glutamine (2 mM), sodium pyruvate (1 mM), penicillin/streptomycin (100 U/mL/100  $\mu\text{g}/\text{mL}$ ), 10 % FBS and a cocktail of insulin (10  $\mu\text{g}/\text{mL}$ ) (Cat. No. I0516, Sigma-Aldrich, St. Louis, MO), 3-isobutyl-1-methylxanthine (IBMX) (500  $\mu\text{M}$ ) (Cat. No. PHZ1124, Invitrogen, Waltham, MA), and dexamethasone (1  $\mu\text{M}$ ) (Cat. No. AAA1759003, Thermo Fisher Scientific, USA). After 48 h, the media was replaced with DMEM with L-glutamine, sodium pyruvate, penicillin/streptomycin, and 10 % FBS as used as differentiation media and insulin (10  $\mu\text{g}/\text{mL}$ ) for another 48 h. The media was further replaced and the cells were maintained in DMEM supplemented with L-glutamine, sodium pyruvate, penicillin/streptomycin, and FBS as in the previous concentration and insulin (2.5  $\mu\text{g}/\text{mL}$ ) until full differentiation. At day 7, the adipocytes were treated with 10  $\mu\text{M}$  PC or without (control). Cell morphology and accumulation of lipid droplets inside the cells were documented with an AMG EVOS FL inverted microscope from Life Technologies. Cell morphological parameters including cell area, perimeter, and circularity were quantified from phase contrast images by ImageJ software (NIH) (Number of cells,  $n = 45$  in each dish).

## 2.3. Annexin V/PI apoptosis assay

Splenocytes were pretreated with PC (10  $\mu\text{M}$  or 50  $\mu\text{M}$ ) for 72 h after anti-CD3 and anti-CD28 stimulation as described above. For detection of apoptosis, stimulated splenocytes ( $1 \times 10^6$ ) were stained with annexin V-conjugated to Alexa Fluor 488 and propidium iodide (PI) by using annexin V/dead cell apoptosis kit (Cat. No. V13242, Invitrogen, Waltham, MA). Briefly, cells were suspended in 100  $\mu\text{L}$  of annexin-binding buffer and incubated with 5  $\mu\text{L}$  of annexin V and 1  $\mu\text{L}$  of 100  $\mu\text{g}/\text{mL}$  PI working solution for 15 min at room temperature RT. After incubation, 400  $\mu\text{L}$  of annexin-binding buffer was added and the stained cells were analyzed by Novocyte flow cytometer (Agilent Technologies, Santa Clara, CA).

## 2.4. Flow cytometry

Compensation beads, isotype controls, and fluorescence-conjugated antibodies were purchased from either BD Bioscience (San Diego, CA) or Biolegend (San Diego, CA). For each experimental study, freshly isolated cells were pelleted and resuspended in 80  $\mu$ L of ice-cold flow cytometry staining buffer (FACS buffer), PBS (Cat. No. 10010-031, Gibco, Waltham, MA) containing 1 % fetal bovine serum (FBS). Later, the cells from each well in triplicate were stained with 5  $\mu$ L of the manufacturer's recommended dilutions of either respective fluorescence-conjugated antibodies or their respective controls at 4°C for 40 min. We used the following fluorescently labeled mouse monoclonal antibodies for flow cytometry: APC-conjugated anti-CD4 (clone: GK1.5), FITC-conjugated anti-CD8 (clone: 53-6.7), PE-conjugated anti-CXCR3 (clone: CXCR3-173), PE-conjugated anti-FoxP3 (clone: MF-14), APC-conjugated anti-IL-6R (clone: D7715A7), PE-conjugated anti-iNOS (clone: W16030C), APC-conjugated anti-TNF- $\alpha$  (clone: MP6-XT22). For intracellular staining (ICS) of FoxP3, IL-6R, iNOS, and TNF- $\alpha$ , the cells were re-suspended in BD Cytofix/Cytoperm solution for 20 min. The cells were again washed with BD perm/wash solution after storage at 4°C for 10 min. Intracellular staining, incubation, and analysis of IL-6R, FoxP3, iNOS, and TNF- $\alpha$  were performed according to the manufacturer's protocol at RT (dark) for 30 min. Afterward, cells were washed with FACS buffer and resuspended in 300  $\mu$ L of FACS buffer. The quantification of fluorescent signals was measured using a Novocyte flow cytometer (Agilent Technologies, Santa Clara, CA), and expressed relative to isotype controls.

## 2.5. Western blot analysis

RAW264.7 cells were seeded into ( $0.5 \times 10^6$  cells/well) 6-well plates and incubated at 37°C along with 5 % CO<sub>2</sub>. After 24 h, cells were treated with 100 ng/mL LPS and with or without 10  $\mu$ M PC. After 24 h of treatment, cells were washed twice with ice-cold PBS and lysed in RIPA buffer (Cat. No. J63306, Alfa Aesar, Haverhill, MA) with protease and phosphatase inhibitors. The cell lysate was centrifuged to collect the supernatant and protein concentration was measured using a BCA protein assay kit (Cat. No. 23225, Thermo Fisher Scientific, Waltham, MA). 20  $\mu$ g of protein from each group were mixed with 4X laemmli buffer (Cat. No. #1610747, Bio-Rad, Hercules, CA) and 2- $\beta$ -mercaptoethanol (Cat. No. A15890, Alfa Aesar, Haverhill, MA), then heated at 95°C for 5 min. The protein samples were resolved and separated by 10 % sodium dodecyl sulfate-polyacrylamide gel electrophoresis (SDS-PAGE) (Bio-Rad, Hercules, CA). Proteins were transferred from the gel to polyvinylidene fluoride (PVDF) membranes (Cat. No. # 1620174, Bio-Rad, Hercules, CA) by using a trans-blot turbo instrument (Bio-Rad, Hercules, CA). Membranes were blocked with intercept blocking buffer (# 92760001, LI-COR Biosciences, Lincoln, NE) at RT for 2 h and were incubated with anti-NF- $\kappa$ B p50 (1:100, # 8414, Santa Cruz Biotechnology, Dallas, TX) and anti- $\beta$ -actin (1:5000, LI-COR Biosciences, Lincoln, NE) primary antibodies overnight at 4°C with continuous shaking. Afterward, the membranes were washed with TBS containing 0.2 % Tween 20 (Cat. No. 28360, Thermo Scientific Fisher, Waltham, MA) 3 times for 5 min. Then, the membranes were incubated with IRDye<sup>®</sup> 800CW-labeled goat anti-mouse IgG (# 926-32210, LI-COR Biosciences, Lincoln, NE), IRDye<sup>®</sup> 680RD-labeled goat anti-mouse IgG (# 925-68070, LI-COR Biosciences, Lincoln, NE), or goat anti-rabbit IgG (# 926-32211, LI-COR Biosciences, Lincoln, NE)

secondary antibodies (1:5000) at RT for 1 h. Images were taken with an LI-COR Odyssey<sup>®</sup> DLX imaging system (LI-COR Biosciences, Lincoln, NE) and densitometry analyses were performed with LI-COR Image Studio Software (LI-COR Biosciences, Lincoln, NE).

## 2.6. Oil red O staining and imaging with quantification

Untreated and 24 h PC-treated differentiated NIH3T3-L1 adipocytes were washed twice with PBS and fixed with 4 % paraformaldehyde for 15 min at RT. Cells were washed with PBS. The fixed cells were stained with freshly diluted Oil Red O (Cat no. 00625, Sigma Aldrich) solution for 45 min at RT, followed by washing thrice with distilled water. Cells were counterstained with Hematoxylin (Cat no. MAK 194 D, Sigma) and mounted. Microphotographs were captured with an Olympus BX43 bright field microscope. The greyscale mean intensity of oil red O stain of oil droplets inside the cell was quantified by ImageJ (number of an oil droplet,  $n = 75$ ). The intensity was normalized by the respective background.

## 2.7. Total RNA isolation and quantitative real-time polymerase chain reaction

Differentiated NIH3T3-L1 cells were treated with or without 10  $\mu$ M PC. Total RNA was extracted using Qiazol (QIAGEN, Germantown, MD) following the manufacturer's instructions. The concentration and purity of the total RNA were determined by NanoDrop (Thermo Fisher Scientific, Waltham, MA). Total RNA (1  $\mu$ g) was converted into cDNA by iScript cDNA synthesis kit (Bio-Rad, Hercules, CA) according to the manufacturer's procedure. The mRNA expression of targeted genes including *leptin* (Forward sequence: GCA GTG CCT ATC CAG AAA GTC C, Reverse sequence: GGA ATG AAG TCC AAG CCA GTG AC, IDT, Coralville, IA), *IL-1 $\beta$*  (Forward sequence: TGG ACC TTC CAG GAT GAG GAC A, Reverse sequence: GTT CAT CTC GGA GCC TGT AGT G, IDT, Coralville, IA), *TNF- $\alpha$*  (Forward sequence: GGT GCC TAT GTC TCA GCC TCT T, Reverse sequence: GCC ATA GAA CTG ATG AGA GGG AG, IDT, Coralville, IA) was measured by quantitative PCR (qPCR) using the appropriate primers and iTaq Universal SYBR Green Supermix (Bio-Rad, Hercules, CA) with a CFX96 Touch<sup>™</sup> Real-Time PCR Detection System (Bio-Rad, Hercules, CA). GAPDH (QIAGEN, Germantown, MD) was used as a reference gene.

## 2.8. Statistical analysis

Data are expressed as the means  $\pm$  standard error of the mean (SEM) for all the experiments. Statistical significance was calculated compared to control groups and determined either by one-way ANOVA or by Student's t-tests.  $p < 0.05$  was considered significant. The experiments were repeated three times in triplicate.

# 3. Results

## 3.1. PC alters the frequency and activation of T cells

It has been shown that activated T cells increased significantly during inflammation and contribute to an inflammatory response by releasing several proinflammatory cytokines [19]. Further, CD8 T cells secrete proinflammatory cytokines due to the abundance of interferon- $\gamma$  producing effector cells [20]. During preliminary studies, we used various doses (1, 5, 10,

50, and 100  $\mu\text{M}$  PC) and determined that the 10  $\mu\text{M}$  dose is the most effective and used in this study (data not shown). However, 50  $\mu\text{M}$  dose that does not produce toxicity was also used for a few experiments in this study. Since naïve, activated, and effector T cells regulate inflammation by different mechanisms, we sought to analyze the effect of PC on the frequency of stimulated splenocytes. The frequency of both CD4 and CD8 decreased after 10  $\mu\text{M}$  PC treatment as compared to the control (Fig. 1A and C). However, we noticed a significant reduction in the CD8 frequency after PC treatment as compared to stimulation alone (13.9 % vs 9.22 %) (Fig. 1A). These results suggest that PC effectively reduces the activation of both T cells with a stronger effect in CD8 T cells.

CXCR3, a chemokine receptor facilitates T-cell differentiation and is increased in inflamed conditions [21]. We further investigated the frequency of CXCR3 after PC treatment. Our results indicated that the frequency of  $\text{CD8}^+\text{CXCR3}^+$  was decreased after PC treatment as compared with that of stimulated splenocytes alone (Fig. 1B and C). These findings indicate that PC reduces the expression of  $\text{CD8}^+\text{CXCR3}^+$  after T-cell activation.

### 3.2. PC induces the frequency of regulatory T cells (Tregs) and apoptosis in activated T cells

The increased frequency and function of Tregs during inflammation plays a pivotal role in controlling inflammation and evidence suggests that Tregs suppress inflammation by suppressing immune response [22]. Thus, we analyzed the frequency of Tregs in the splenocytes after PC treatment using flow cytometry. The stimulated splenocytes showed an increase in the frequency of Tregs as compared with the control group (Fig. 2A). Interestingly, we also noticed that PC further induces the frequency of Tregs as compared to the stimulated group alone. We also used a higher dose of 50  $\mu\text{M}$  PC and noticed that Tregs were even more increased after PC treatment (Fig. 2A). These results suggest that PC might be used for the inhibitory effect on inflammation through the induction of Tregs.

Apoptosis is a key step in reducing the inflammatory immune response, and the number of activated T cells decreases significantly during the suppression of inflammation [23]. Thus, we also analyzed the effect of PC on apoptosis in activated T cells by flow cytometry. We noticed an increase in stimulated T-cell apoptosis after PC treatment as compared to the control. We noticed 13.5 % apoptotic cells increased to 28.1 % in the 50  $\mu\text{M}$  PC treated as compared to the stimulated group alone (Fig. 2B). After treatment with PC, the frequency of apoptotic cells was dramatically increased in a dose-dependent manner. These data indicated that PC successfully induces apoptosis in activated T cells as compared to control.

### 3.3. PC reduces the inflammatory response in LPS-induced RAW264.7 macrophage

Inflammation is a complex response and mounting evidence suggests that  $\text{TNF-}\alpha$ , IL-6, and inducible nitric oxide synthase (iNOS) are over-produced and secreted during a variety of inflammatory disorders [24]. Hence, we determined whether PC treatment reduces these cytokines in the LPS-induced RAW264.7 macrophage. Our results delineated that after LPS treatment, the frequency of  $\text{TNF-}\alpha$ , iNOS, and IL-6R increased percentages of 46.45 %, 24.52 %, and 7.23 % respectively (Fig. 3A). PC treatment decreased the frequency of  $\text{TNF-}\alpha$ , iNOS, and IL-6R in the LPS-induced RAW264.7 cell line to 30.39 %, 7.52 %, and

4.29 % respectively (Fig. 3A). Thus, PC treatment was able to decrease the responses of inflammatory cytokines in the LPS-induced RAW264.7 macrophages.

#### **3.4. PC reduces the expression of cytokines and NF- $\kappa$ B in LPS-induced RAW264.7 macrophage**

LPS induction in macrophages leads to the production of several proinflammatory markers, including IL-1 $\beta$ , TNF- $\alpha$ , and IL-6 [25]. We analyzed the LPS-induced morphological changes in response to PC treatment and noticed an increase in size as well as obvious proliferation and several irregular pseudopods, which indicates that LPS-induced inflammation leads to abnormal proliferation of RAW264.7 macrophages (Fig. 4A). However, PC treatment resulted in the reduction of cell density and attenuated the abnormal proliferation (Fig. 4A). These results suggest that PC treatment altered the morphology of RAW264.7 macrophages after LPS induction.

NF- $\kappa$ B is considered a ubiquitous transcription factor and regulates the expression of a large array of genes that are involved in different processes related to immune as well as inflammatory responses [26]. Further, it has been shown that activation of NF- $\kappa$ B by LPS induces plenty of proinflammatory mediators [27]. Thus, we investigated the possible suppressive effects of PC on the activation of NF- $\kappa$ B in LPS-induced RAW264.7 macrophages. LPS treatment significantly increased the expression of NF- $\kappa$ B compared to the control group (Fig. 4B and C). On the other hand, PC treatment caused a reduction in the protein expression of NF- $\kappa$ B when compared with the LPS-alone group (Fig. 4B and C). These results suggested that the inhibition of translocation of NF- $\kappa$ B by PC might be the mechanism that leads to the suppression of several proinflammatory mediators, including TNF- $\alpha$ , IL-6, and iNOS.

#### **3.5. PC alters NIH3T3-L1 cell morphology, lipid accumulation, and gene expression**

To assess the effect of PC on adipocytes, we evaluated and compared the cell morphology, lipid deposition, and the expression of IL-1 $\beta$ , TNF- $\alpha$ , and leptin in NIH3T3-L1 adipocytes. After treating these cells with PC, the cell size was reduced in the PC-treated group which was reflected in cell area and perimeter (Fig. 5A and B). Interestingly, PC-treated cells became morphologically more round in shape compared to the control group because the circularity parameter increased (circularity is the ratio of area to the perimeter). Furthermore, in the PC-treated group, the oil droplets were dispersed in the cytoplasm whereas the oil droplets are very densely packed and covered the whole cytoplasm in the control group (Fig. 5A **red and yellow arrows**). This difference is further validated by measuring the intensity of oil red O on stained bright field images (40X). There was a significant reduction in the intensity of oil droplets in the treated cell compared to the control (Fig. 5B). Furthermore, the expression of TNF- $\alpha$  was reduced significantly (Fig. 5C). However, the gene expression for leptin was increased after PC administration and IL-1 $\beta$  also showed a similar pattern (Fig. 5C). The results suggested that PC reduced the hypertrophy of adipocytes and also decreased inflammation, which may indicate that PC has an anti-adipogenic effect.



## 4. Discussion

Drug discovery using natural products remains an area of huge opportunity, as there are centuries of historical knowledge describing the benefits of nature providing considerable remedial and synergistic effects. However, new strategies need to be explored to identify new moieties in these compounds and their mechanism of action to promote their therapeutic effects. Normally, these natural compounds are safe, have minimal toxicity, and are without any adverse side effects. One example is resveratrol, which is widely considered an anticancer, anti-oxidant, and anti-inflammatory, but represents low bioavailability and rapid metabolism [28]. To overcome this issue, PC, a derivative of resveratrol has been reported to have great potential to suppress inflammation [29]. However, the mechanism of the suppressive properties of PC is not clear. In this study, we demonstrated that PC exhibited multifactorial effects. First, PC increased the frequency of Tregs and T cell apoptosis. Second, PC reduced the expression of CXCR3 on T cells, and the levels of TNF- $\alpha$ , IL-6R, NF- $\kappa$ B, and iNOS in RAW264.7 macrophages. Third, PC decreased the hypertrophy of adipocytes in 3T3-L1 adipocytes.

Inflammation is considered a pathological cause of various diseases and seriously endangers human health around the globe. Immune cells play a key role in maintaining the regulation of inflammation and are the mediator for the progression of disease symptoms. Both CD4 and CD8 T cells are recruited to the sites of inflammation during inflammatory diseases [30]. In the present in vitro study, we noticed that PC reduces the frequency of T cells in anti-CD3 and anti-CD28 stimulated splenocytes. These findings corroborated the results from a previous study where PC inhibited the activation markers in both CD4 and CD8 T cells [31]. It has been shown that type 1 helper (Th1) cells are elevated during chronic inflammation [32], and CXCR3-expressing T cells mediate Th1 inflammatory lymphocytes [33]. We also observed that PC decreased the frequency of CXCR3-expressing CD8 T cells, which may have resulted from the inhibition of activated T cells. Prior work has demonstrated that Tregs were immunosuppressors and suppressed the activation of various immune cells, including T and B cells, natural killers, and dendritic cells. Further, an increase in Tregs is considered a key regulator of several types of immune response [34]. In our study, PC treatment increased the frequency of Tregs, which confirms a previous finding that increased Tregs mediate the apoptosis of T cells [35]. Furthermore, the decrease in CXCR3<sup>+</sup> T cells is also plausible by indirectly inducing Tregs, which is associated with the suppression of inflammatory responses to maintain immune homeostasis [36]. We also demonstrated that PC induces apoptosis in the activated T cells and further influences the functional sub-type of T cell response.

When considering other immune cells, LPS-stimulated RAW264.7 macrophages are used as the model for inflammation [37,38]. Inflammation-induced by activated macrophages makes both NO and iNOS an important markers for inflammatory response [39]. Our findings would suggest that the loss of iNOS expression following exposure to PC in the LPS-treated RAW264.7 macrophages may explain the anti-inflammatory effects of PC. In this study, we noticed that LPS increased the expression of iNOS in RAW264.7 macrophages as compared to the control. Treatment with PC drastically decreased the iNOS expression. Additionally, it has been shown that proinflammatory cytokines, such as TNF- $\alpha$  and IL-6R, are responsible

for various inflammatory disorders [40]. In confirmation of these prior observations, we detected a reduction in both TNF- $\alpha$  and IL-6R in RAW264.7 macrophages treated with PC. Taken together, our results corroborate that PC reduces the proinflammatory markers during the LPS-induced inflammatory response. Additionally, these findings corroborated previous studies that demonstrated the role of PC in decreased expression of proinflammatory markers [13,41].

NF- $\kappa$ B is a transcription factor associated with the regulation of several proinflammatory genes, including TNF- $\alpha$ , iNOS, IL-6, and IL-1 $\beta$  [42]. Hence, modulation of NF- $\kappa$ B activity is considered a crucial target for developing an anti-inflammatory drug. Growing evidence suggested that macrophage-mediated inflammatory responses also include the NF- $\kappa$ B signaling pathway [43]. In this study, LPS-stimulated macrophages showed a marked increase in the expression of NF- $\kappa$ B, as well as a significant increase in the level of proinflammatory cytokines, including TNF- $\alpha$ , iNOS, and IL-6R. Conversely, concomitant treatment of PC represented an anti-inflammatory effect by decreasing the expression of NF- $\kappa$ B and inflammatory markers. In addition, the anti-inflammatory effect of PC has been reported in previous studies, thereby providing significant hints regarding the role of PC as an anti-inflammatory therapeutic agent [26,44,45].

Adipose tissue stores lipids by enlarging existing adipocytes as well as recruitment of new adipocytes so that it can accommodate excess lipids, known as hypertrophy and hyperplasia respectively [46]. It has been shown that the anti-adipogenic effect of PC is more significant compared to resveratrol [47]. Moreover, the effect of PC in inhibiting adipogenesis followed dose-dependently in NIH3T3-L1 adipocytes [8]. One reason for the protective effect of PC for negatively regulating adipogenesis is that it reduces various proinflammatory markers. In the present study, we demonstrated that PC significantly reduced the cell size, oil droplet density, deposition, TNF- $\alpha$  expression. Nonetheless, previous studies showed that leptin is directly associated with the inhibition of lipogenesis and promotes lipolysis by acting directly on adipocytes [48]. This leptin activity might be due to the suppression of the inhibitory action of adenylyl cyclase [49]. Previous studies suggested that PC regulates adipocyte differentiation [8,13,17]. By contrast, our study investigated the effect of PC after adipocyte differentiation. Interestingly, the outcomes depicted that PC diminishes the hypertrophy of mature adipocytes, lipid accumulation inside the cell and minimizes the and expression of the proinflammatory gene. Additionally, PC alters the adipocyte shape from elongated to a more-round shape which might indicate the role of PC on any mechanosensory receptors on mature adipocytes. It has been shown that various mechanosensory proteins regulate cell morphology [50]. However, we need further investigation to make a definitive conclusion on how PC alters adipocytes after differentiation.

## 5. Conclusion

Our findings strongly demonstrate that PC induces the frequency of Tregs and apoptosis in the activated splenocytes. PC also decreases the expression of several proinflammatory mediators in immune cells as well as in adipocytes. Additionally, PC regulates adipocyte shape, size, and lipid deposition. Taken together, our study reveals the anti-inflammatory,

anti-adipogenic, and apoptotic activities of PC. This provides a suitable scope for subsequent *in vivo* investigation of PC to confirm its potential health benefits and utility as a treatment modality in various inflammatory diseases and obesity.

## Acknowledgments

This study was supported by grants from National Institute of Allergy and Infectious Diseases, USA (NIAID R01 AI140405) to the U.S., and the Intramural Research Program, UTHSC in Memphis, TN.

## Data availability

Data will be made available on request.

## References

- [1]. Banik K, Ranaware AM, Harsha C, Nitesh T, Girisa S, Deshpande V, et al. , Piceatannol: a natural stilbene for the prevention and treatment of cancer, *Pharmacol. Res* 153 (2020), 104635. [PubMed: 31926274]
- [2]. Piotrowska H, Kucinska M, Murias M, Biological activity of piceatannol: leaving the shadow of resveratrol, *Mutat. Res. /Rev. Mutat. Res* 750 (1) (2012) 60–82.
- [3]. Wen J, Lin H, Zhao M, Tao L, Yang Y, Xu X, et al. , Piceatannol attenuates D-GalN/LPS-induced hepatotoxicity in mice: involvement of ER stress, inflammation and oxidative stress, *Int. Immunopharmacol* 64 (2018) 131–139. [PubMed: 30173053]
- [4]. Fei Y, Wang J, Peng B, Peng J, Hu J-H, Zeng Z-P, et al. , Phenolic constituents from *Rheum nobile* and their antioxidant activity, *Nat. Prod. Res* 31 (24) (2017) 2842–2849. [PubMed: 28301949]
- [5]. Kershaw J, Kim K-H, The therapeutic potential of piceatannol, a natural stilbene, in metabolic diseases: a review, *J. Med. Food* 20 (5) (2017) 427–438. [PubMed: 28387565]
- [6]. Li Y, Yang P, Chang Q, Wang J, Liu J, Lv Y, et al. , Inhibitory effect of piceatannol on TNF- $\alpha$ -mediated inflammation and insulin resistance in 3T3-L1 adipocytes, *J. Agric. Food Chem* 65 (23) (2017) 4634–4641. [PubMed: 28535046]
- [7]. Tung Y-C, Lin Y-H, Chen H-J, Chou S-C, Cheng A-C, Kalyanam N, et al. , Piceatannol exerts anti-obesity effects in C57BL/6 mice through modulating adipogenic proteins and gut microbiota, *Molecules* 21 (11) (2016) 1419. [PubMed: 27792146]
- [8]. Kwon JY, Seo SG, Heo Y-S, Yue S, Cheng J-X, Lee KW, et al. , Piceatannol, natural polyphenolic stilbene, inhibits adipogenesis via modulation of mitotic clonal expansion and insulin receptor-dependent insulin signaling in early phase of differentiation, *J. Biol. Chem* 287 (14) (2012) 11566–11578. [PubMed: 22298784]
- [9]. Xiang P, Chen T, Mou Y, Wu H, Xie P, Lu G, et al. , NZ suppresses TLR4/NF- $\kappa$ B signalings and NLRP3 inflammasome activation in LPS-induced RAW264. 7 macrophages, *Inflamm. Res* 64 (10) (2015) 799–808. [PubMed: 26298161]
- [10]. Lucas J, Hsieh T-C, Halicka HD, Darzynkiewicz Z, Wu JM, Upregulation of PD-L1 expression by resveratrol and piceatannol in breast and colorectal cancer cells occurs via HDAC3/p300-mediated NF- $\kappa$ B signaling, *Int. J. Oncol* 53 (4) (2018) 1469–1480. [PubMed: 30066852]
- [11]. Maruki-Uchida H, Morita M, Yonei Y, Sai M, Effect of passion fruit seed extract rich in piceatannol on the skin of women: a randomized, placebo-controlled, double-blind trial, *J. Nutr. Sci. Vitaminol* 64 (1) (2018) 75–80. [PubMed: 29491276]
- [12]. Chawla A, Nguyen KD, Goh Y, Macrophage-mediated inflammation in metabolic disease, *Nat. Rev. Immunol* 11 (11) (2011) 738–749. [PubMed: 21984069]
- [13]. Yamamoto T, Li Y, Hanafusa Y, Yeh YS, Maruki-Uchida H, Kawakami S, et al. , Piceatannol exhibits anti-inflammatory effects on macrophages interacting with adipocytes, *Food Sci. Nutr* 5 (1) (2017) 76–85. [PubMed: 28070318]
- [14]. Juhas U, Ryba-Stanisławowska M, Szargiej P, Mysłowska J, Different pathways of macrophage activation and polarization, *Adv. Hyg. Exp. Med./Post. Hig. i Med. Doswiadczalnej* 69 (2015).

- [15]. Liu T, Zhang L, Joo D, Sun S-C, NF- $\kappa$ B signaling in inflammation, *Signal Transduct. Target. Ther* 2 (1) (2017) 1–9.
- [16]. Fathy M, Khalifa EM, Fawzy MA, Modulation of inducible nitric oxide synthase pathway by eugenol and telmisartan in carbon tetrachloride-induced liver injury in rats, *Life Sci* 216 (2019) 207–214. [PubMed: 30452970]
- [17]. Kwon JY, Kershaw J, Chen C-Y, Komanetsky SM, Zhu Y, Guo X, et al. , Piceatannol antagonizes lipolysis by promoting autophagy-lysosome-dependent degradation of lipolytic protein clusters in adipocytes, *J. Nutr. Biochem* 105 (2022), 108998. [PubMed: 35346829]
- [18]. Duncan RE, Ahmadian M, Jaworski K, Sarkadi-Nagy E, Sul HS, Regulation of lipolysis in adipocytes, *Annu. Rev. Nutr* 27 (2007) 79. [PubMed: 17313320]
- [19]. Kiran S, Rakib A, Singh UP, The NLRP3 inflammasome inhibitor dapansutril attenuates cyclophosphamide-induced interstitial cystitis, *Front. Immunol* 13 (2022).
- [20]. Skapenko A, Leipe J, Lipsky PE, Schulze-Koops H, The role of the T cell in autoimmune inflammation, *Arthritis Res. Ther* 7 (2) (2005) 1–11. [PubMed: 15642148]
- [21]. Groom JR, Luster AD, CXCR3 in T cell function, *Exp. Cell Res* 317 (5) (2011) 620–631. [PubMed: 21376175]
- [22]. Shevach EM, Mechanisms of foxp3+ T regulatory cell-mediated suppression, *Immunity* 30 (5) (2009) 636–645. [PubMed: 19464986]
- [23]. Hacker G, A. Bauer, A. Villunger, Apoptosis in activated T cells—what are the triggers, and what the signal transducers? *Cell Cycle* 5 (21) (2006) 2421–2424. [PubMed: 17102629]
- [24]. Singh UP, Singh NP, Singh B, Hofseth LJ, Taub DD, Price RL, et al. , Role of resveratrol-induced CD11b+ Gr-1+ myeloid derived suppressor cells (MDSCs) in the reduction of CXCR3+ T cells and amelioration of chronic colitis in IL-10<sup>-/-</sup> mice, *Brain, Behav., Immun* 26 (1) (2012) 72–82. [PubMed: 21807089]
- [25]. Cho J-S, Kang J-H, Um J-Y, Han I-H, Park I-H, Lee H-M, Lipopolysaccharide induces pro-inflammatory cytokines and MMP production via TLR4 in nasal polyepidermal fibroblast and organ culture, *PLoS One* 9 (11) (2014), e90683. [PubMed: 25390332]
- [26]. Youn J, Lee J-S, Na H-K, Kundu JK, Surh Y-J, Resveratrol and piceatannol inhibit iNOS expression and NF- $\kappa$ B activation in dextran sulfate sodium-induced mouse colitis, *Nutr. Cancer* 61 (6) (2009) 847–854. [PubMed: 20155626]
- [27]. Guha M, Mackman N, LPS induction of gene expression in human monocytes, *Cell. Signal* 13 (2) (2001) 85–94. [PubMed: 11257452]
- [28]. Ding S, Jiang H, Fang J, Liu G, Regulatory effect of resveratrol on inflammation induced by lipopolysaccharides via reprogramming intestinal microbes and ameliorating serum metabolism profiles, *Front. Immunol* (2021) 4568.
- [29]. Gao X, Kang X, Lu H, Xue E, Chen R, Pan J, et al. , Piceatannol suppresses inflammation and promotes apoptosis in rheumatoid arthritis-fibroblast-like synoviocytes by inhibiting the NF- $\kappa$ B and MAPK signaling pathways, *Mol. Med. Rep* 25 (5) (2022) 1–10. [PubMed: 34726254]
- [30]. Rauch D, Gross S, Harding J, Bokhari S, Niewiesk S, Lairmore M, et al. , T-cell activation promotes tumorigenesis in inflammation-associated cancer, *Retrovirology* 6 (1) (2009) 1–10. [PubMed: 19128510]
- [31]. Singh UP, Singh NP, Singh B, Hofseth LJ, Price RL, Nagarkatti M, et al. , Resveratrol (trans-3, 5, 4'-trihydroxystilbene) induces silent mating type information regulation-1 and down-regulates nuclear transcription factor- $\kappa$ B activation to abrogate dextran sulfate sodium-induced colitis, *J. Pharmacol. Exp. Ther* 332 (3) (2010) 829–839. [PubMed: 19940103]
- [32]. Benaglio M, Azzurri A, Ciervo A, Amedei A, Tamburini C, Ferrari M, et al. , T helper type 1 lymphocytes drive inflammation in human atherosclerotic lesions, *Proc. Natl. Acad. Sci* 100 (11) (2003) 6658–6663. [PubMed: 12740434]
- [33]. Bonocchi R, Bianchi G, Bordignon PP, D'Ambrosio D, Lang R, Borsatti A, et al. , Differential expression of chemokine receptors and chemotactic responsiveness of type 1 T helper cells (Th1s) and Th2s, *J. Exp. Med* 187 (1) (1998) 129–134. [PubMed: 9419219]
- [34]. Glaubitz J, Wilden A, Golchert J, Homuth G, Volker U, Bröker BM, et al. , In mouse chronic pancreatitis CD25+ FOXP3+ regulatory T cells control pancreatic fibrosis by suppression of the type 2 immune response, *Nat. Commun* 13 (1) (2022) 1–20. [PubMed: 34983933]

- [35]. Pandiyan P, Zheng L, Ishihara S, Reed J, Lenardo MJ, CD4+ CD25+ Foxp3+ regulatory T cells induce cytokine deprivation-mediated apoptosis of effector CD4 + T cells, *Nat. Immunol* 8 (12) (2007) 1353–1362. [PubMed: 17982458]
- [36]. Littman DR, Rudensky AY, Th17 and regulatory T cells in mediating and restraining inflammation, *Cell* 140 (6) (2010) 845–858. [PubMed: 20303875]
- [37]. Tan Y, Zhang X, Cheang WS, Isoflavones daidzin and daidzein inhibit lipopolysaccharide-induced inflammation in RAW264. 7 macrophages, *Chin. Med* 17 (1) (2022) 1–10.
- [38]. Abusaliya A, Bhosale PB, Kim HH, Ha SE, Park MY, Jeong SH, et al. . Prunetinoside inhibits lipopolysaccharide-provoked inflammatory response via suppressing NF- $\kappa$ B and activating the JNK-mediated signaling pathway in RAW264. 7 macrophage cells, *Int. J. Mol. Sci* 23 (10) (2022) 5442. [PubMed: 35628252]
- [39]. Cirino G, Distrutti E, Wallace JL, Nitric oxide and inflammation, *Inflamm. Allergy-Drug Targets* 5 (2) (2006) 115–119. [PubMed: 16613570]
- [40]. Hirano T, IL-6 in inflammation, autoimmunity and cancer, *Int. Immunol* 33 (3) (2021) 127–148. [PubMed: 33337480]
- [41]. Jin C-Y, Moon D-O, Lee K-J, Kim M-O, Lee J-D, Choi YH, et al. , Piceatannol attenuates lipopolysaccharide-induced NF- $\kappa$ B activation and NF- $\kappa$ B-related proinflammatory mediators in BV2 microglia, *Pharmacol. Res* 54 (6) (2006) 461–467. [PubMed: 17067811]
- [42]. Bellezza I, Mierla AL, Minelli A, Nrf2 and NF- $\kappa$ B and their concerted modulation in cancer pathogenesis and progression, *Cancers* 2 (2) (2010) 483–497. [PubMed: 24281078]
- [43]. Dorrington MG, Fraser ID, NF- $\kappa$ B signaling in macrophages: dynamics, crosstalk, and signal integration, *Front. Immunol* 10 (2019) 705. [PubMed: 31024544]
- [44]. Son P-S, Park S-A, Na H-K, Jue D-M, Kim S, Surh Y-J, Piceatannol, a catechol-type polyphenol, inhibits phorbol ester-induced NF- $\kappa$ B activation and cyclooxygenase-2 expression in human breast epithelial cells: cysteine 179 of IKK $\beta$  as a potential target, *Carcinogenesis* 31 (8) (2010) 1442–1449. [PubMed: 20584749]
- [45]. Tambuwala MM, Khan MN, Thompson P, McCarron PA, Albumin nanoencapsulation of caffeic acid phenethyl ester and piceatannol potentiated its ability to modulate HIF and NF-kB pathways and improves therapeutic outcome in experimental colitis, *Drug Deliv. Transl. Res* 9 (1) (2019) 14–24. [PubMed: 30430451]
- [46]. Drolet R, Richard C, Sniderman A, Mailloux J, Fortier M, Huot C, et al. , Hypertrophy and hyperplasia of abdominal adipose tissues in women, *Int. J. Obes* 32 (2) (2008) 283–291.
- [47]. Park IS, Han Y, Jo H, Lee KW, Song YS, Piceatannol is superior to resveratrol at suppressing adipogenesis in human visceral adipose-derived stem cells, *Plants* 10 (2) (2021) 366. [PubMed: 33672932]
- [48]. William W, Ceddia R, Curi R, Leptin controls the fate of fatty acids in isolated rat white adipocytes, *J. Endocrinol* 175 (3) (2002) 735–744. [PubMed: 12475384]
- [49]. Assinder SJ, Boumelhem BB, Oxytocin stimulates lipolysis, prostaglandin E2 synthesis, and leptin secretion in 3T3-L1 adipocytes, *Mol. Cell. Endocrinol* 534 (2021), 111381. [PubMed: 34216640]
- [50]. Wolfenson H, Yang B, Sheetz MP, Steps in mechanotransduction pathways that control cell morphology, *Annu. Rev. Physiol* 81 (2019) 585. [PubMed: 30403543]

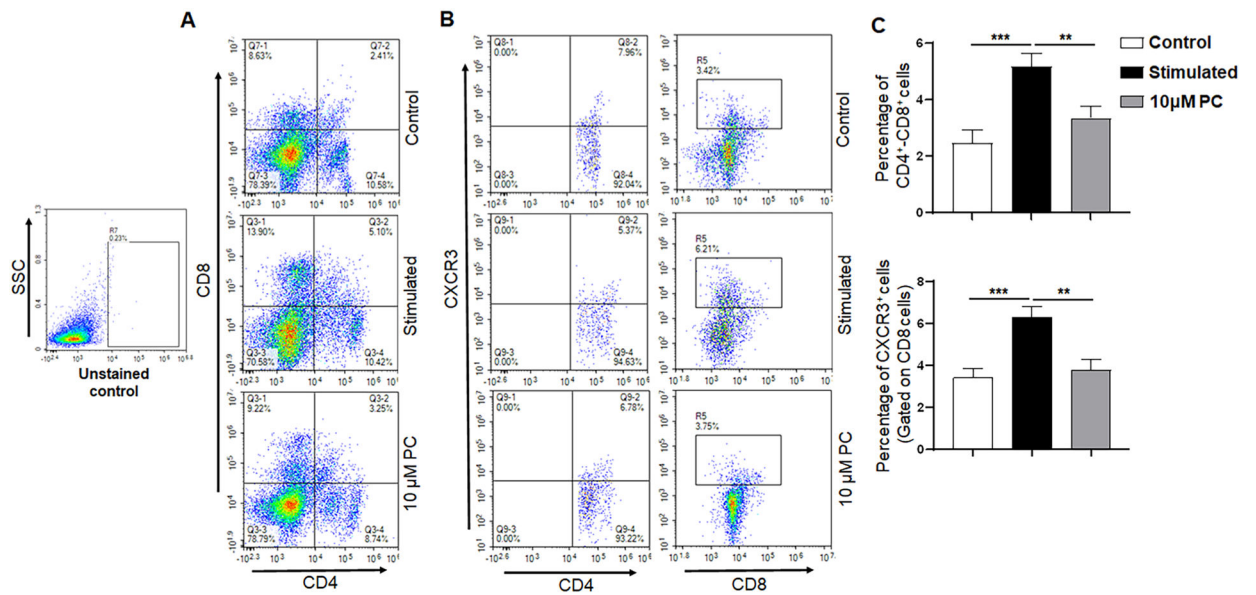


**Fig. 1. PC alters the T cell frequency and reduces activated T cells.**

Flow cytometry analysis of control stimulated, and 10  $\mu\text{M}$  PC treated spleen cells stained with phenotypic markers for T cells (CD4 and CD8) and T cell activation markers CXCR3. **Panel A** represents the percentages of CD4<sup>+</sup> T cells (Panel A, lower right quadrant), CD8<sup>+</sup> T cells (Panel A, upper left quadrant), and CD4<sup>+</sup>CD8<sup>+</sup> T cells (Panel A, upper right quadrant). **Panel B** shows representative experiments for both CD4 +CXCR3 and CD8 +CXCR3 populations. **Panel C** represents the percentages of CD4<sup>+</sup>CD8<sup>+</sup> T cells and CXCR3 cells that were gated on the CD8 T cell population. Data are representative of one of the three biological experiments run in triplicate. The values are shown as mean  $\pm$  SEM; \*  $p < 0.01$  (compared to control vs stimulated); \* \*  $p < 0.001$  (compared to stimulated vs PC).

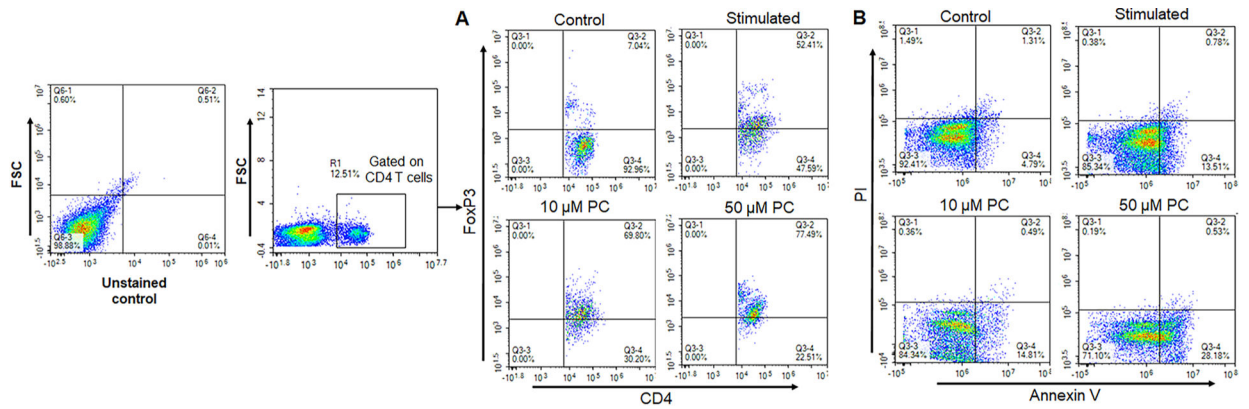


**Fig. 2. PC induces regulatory T cells (Tregs) and induces apoptosis in activated T cells.** Flow cytometry analysis of control, stimulated, 10  $\mu$ M & 50  $\mu$ M PC treated spleen cells, respectively, and stained for CD4, FoxP3 antibodies for Tregs and Annexin V/PI staining for apoptosis analysis. **Panel A** represents the changes in the frequency of FoxP3<sup>+</sup> cells gated on CD4 T cells. **Panel B** shows the apoptosis analysis by Annexin V/PI staining. Data are representative of one of the three biological experiments run in triplicate.

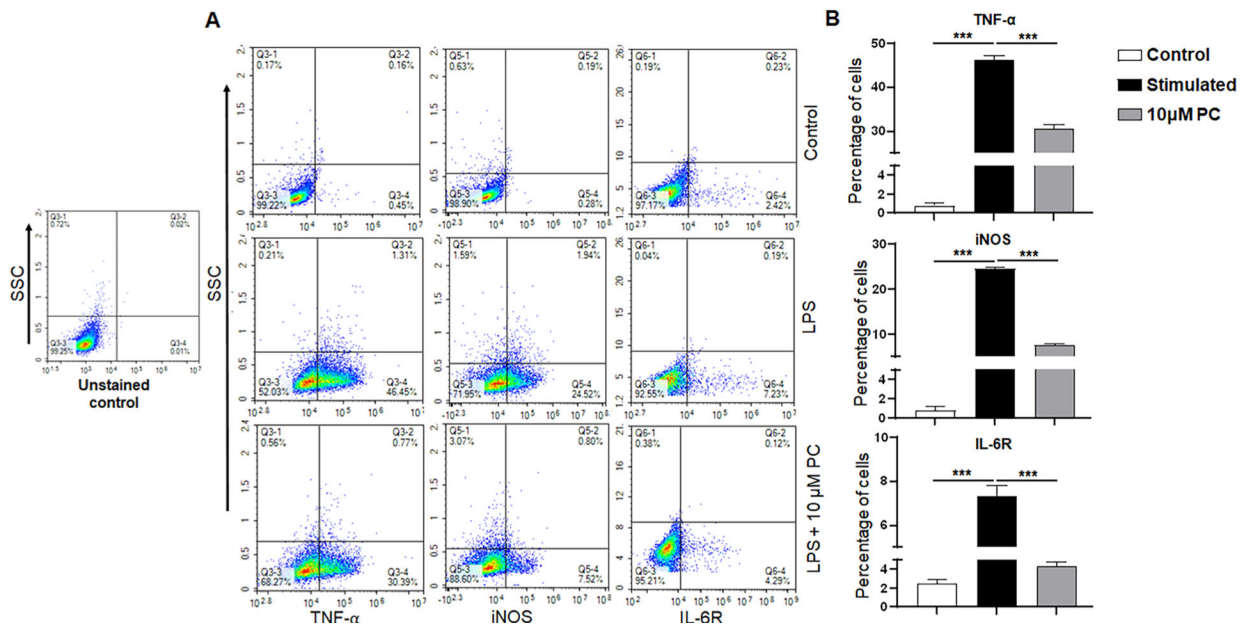


**Fig. 3. Effect of PC on inflammatory mediators in RAW264.7 macrophages.**

RAW264.7 macrophages were treated with 10 μM PC and control in presence of LPS stimulation. Cells were intracellularly stained with TNF-α, iNOS, and IL-6R antibodies. **Panel A** shows the changes in the frequency of TNF-α, iNOS, and IL-6R in control, LPS, and LPS treated with 10 μM PC. **Panel B** shows the percentages of cells in each group for TNF-α, iNOS, and IL-6R. Data are representative of one of the three biological experiments run in triplicate. The values are shown as mean ± SEM; \*\*\**p* < 0.001 (compared to control vs stimulated vs PC).



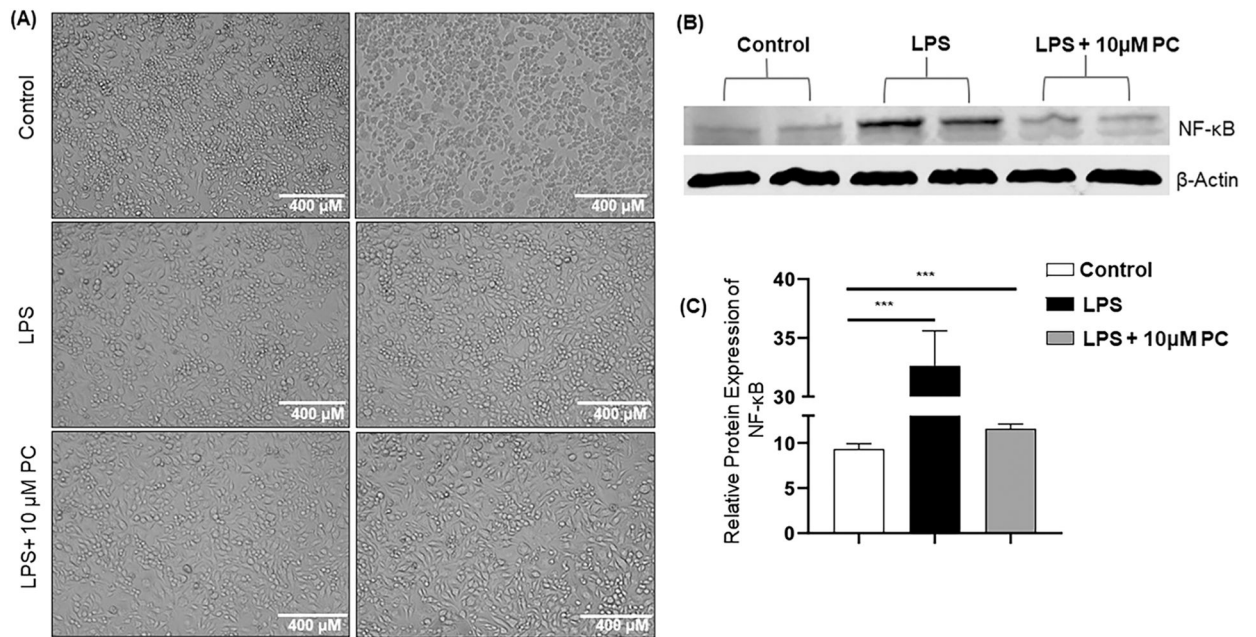


**Fig. 4. PC alters the morphology and expression of NF- $\kappa$ B in LPS-induced RAW264.7 macrophages.**Panel

**A** represents the altered morphology in RAW264.7 cells stimulated with LPS and 10  $\mu$ M PC treatment. **Panel B** shows the expression of NF- $\kappa$ B in RAW264.7 macrophages treated with 10  $\mu$ M PC or control in presence of LPS induction. **Panel C** delineates the relative protein expression of NF- $\kappa$ B normalized with  $\beta$ -actin. Data are representative of one of the three biological experiments run in triplicate. The values are shown as mean  $\pm$  SEM; \*\*\* $p < 0.001$ (compared to control vs stimulated vs PC).

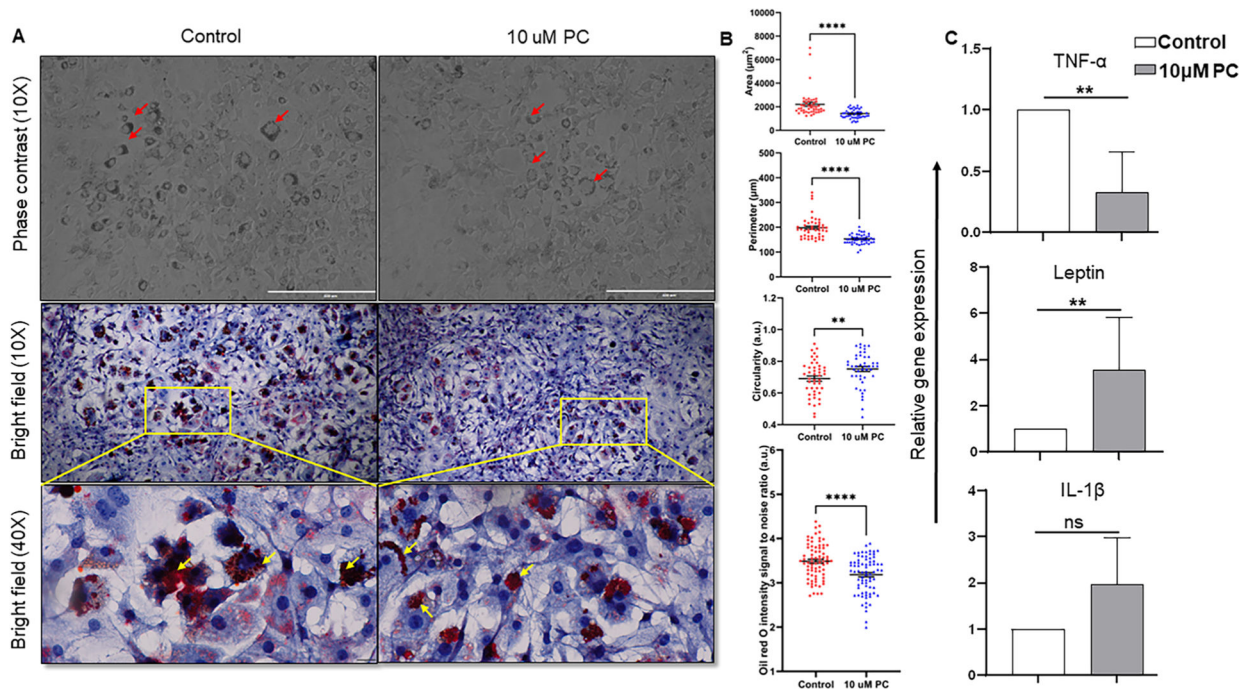


**Fig. 5. Representation of the alteration in morphology, lipid accumulation, and gene expression of 3T3-L1 cells treated with PC.**

A) microphotograph (100X) of cell morphology in phase contrast microscope and microphotograph (100X and 400X) of oil red O-stained cells in bright field microscope, red color represents the lipid accumulation portion inside the cells (Red and yellow arrowheads indicate the difference in lipid deposition between control and treated group in different microscopic modes). B) Graphical illustration of morphometric analysis such as cellular area, perimeter, and circularity ( $n = 45$ ) and oil red O staining intensity ( $n = 75$ ). C) Relative gene expression of TNF- $\alpha$ , leptin, and IL-1 $\beta$ . Data are representative of one of the three biological experiments run in triplicate. The values are shown as mean  $\pm$  SEM; not significant (ns)  $p > 0.05$ , \* $p < 0.05$ , \*\* $p < 0.01$ ; \*\*\* $p < 0.001$ .